

# Structural and magnetic stabilities of cubic and orthorhombic phases of CeMnNi<sub>4</sub>

著者	川添 良幸
journal or publication title	Applied Physics Letters
volume	89
number	22
page range	222502-1-222502-3
year	2006
URL	<a href="http://hdl.handle.net/10097/47052">http://hdl.handle.net/10097/47052</a>

doi: 10.1063/1.2390656

## Structural and magnetic stabilities of cubic and orthorhombic phases of CeMnNi<sub>4</sub>

P. Murugan<sup>a)</sup> and Abhishek Kumar Singh

*Institute for Materials Research, Tohoku University, Aoba-ku, Sendai 980-8577, Japan*

G. P. Das

*Indian Association for the Cultivation of Science, Jadavpur, Kolkata 700032, India*

Yoshiyuki Kawazoe

*Institute for Materials Research, Tohoku University, Aoba-ku, Sendai 980 8577, Japan*

(Received 22 June 2006; accepted 6 October 2006; published online 28 November 2006)

First-principles density functional calculations have been carried out on cubic and orthorhombic phases of CeMnNi<sub>4</sub>, in order to understand their structural and magnetic stabilities. The calculations show the orthorhombic phase to be energetically favorable as compared to the cubic phase reported experimentally by Singh *et al.* [Appl. Phys. Lett. **88**, 022506 (2005)]. Ferromagnetic state turns out to be more stable for both cubic and orthorhombic phases, the latter having lower total magnetic moment. The moment is mainly localized on Mn atoms, and their alignment is mediated via the indirect exchange interaction. Half-metallic nature as proposed experimentally is elusive for the pure compound which shows metallic behavior. © 2006 American Institute of Physics.

[DOI: 10.1063/1.2390656]

Recent experimental study on cubic phase of CeMnNi<sub>4</sub> (Ref. 1) shows that this material can be potentially useful for fabrication of spintronic devices, as it exhibits a large magnetic moment of  $\sim 4.95\mu_B/\text{Mn}$  atom with a high degree of spin polarization. Such high degree of transport spin polarization ( $\approx 66\%$ ) of this intermetallic compound has been observed in point-contact Andreev reflection (PCAR) experiment. First-principles calculations<sup>2,3</sup> carried out on cubic CeMnNi<sub>4</sub> successfully explain the ferromagnetic ground state as well as the large magnetic moment that is predominantly contributed by Mn atoms. However, the calculated values for the transport spin polarization underestimate the experimental observation.<sup>1</sup> This discrepancy has been attributed to possible off stoichiometry and/or disorder in the cubic phase of CeMnNi<sub>4</sub>.<sup>2,3</sup>

CeMnNi<sub>4</sub> is derived from CeNi<sub>5</sub>, which is a well known Pauli paramagnetic system that crystallizes in hexagonal structure with space group 191 (*P6/mmm*). The transition metal element Mn or Fe or Cu dissolves in CeNi<sub>5</sub>,<sup>4</sup> and all these compounds exhibit ferromagnetism.<sup>1,5,6</sup> Even addition of a nontransition metal element Ga into CeNi<sub>5</sub> takes the system close to the paramagnetic-itinerant ferromagnetic state.<sup>7</sup> In particular, CeMn<sub>x</sub>Ni<sub>5-x</sub> ( $x=0.75$ ) compound in hexagonal phase was observed to be ferromagnetic with moment of  $0.42\mu_B/\text{f.u.}$ <sup>5</sup> This magnetic moment is much lower in magnitude compared to that of cubic CeMnNi<sub>5</sub> as reported in the recent experiment.<sup>1</sup> However, both phases exhibit almost similar transition temperature of  $\sim 140$  K.<sup>1,5</sup> The magnetic and structural stabilities of the hexagonal phase have not been completely understood. As Mn concentration increases from  $x=0.75$  to 1.00, one cannot rule out the possibility of stabilization of the hexagonal phase. Moreover, there are other intermetallics in this family that have been synthesized and found to be in hexagonal phase.<sup>8</sup> Hence, we have carried out first-principles density functional investigation of the

hexagonal phase of CeMnNi<sub>4</sub> (actually, the structure becomes orthorhombic, as will be explained later) and compared it with those of the experimentally observed cubic phase. The structural stabilities of both cubic and orthorhombic phases have been studied by total energy calculations with varying lattice parameters. Our calculations reveal that the orthorhombic phase of CeMnNi<sub>4</sub> is energetically favorable as compared to the experimentally observed cubic phase, while for both the structures the ferromagnetic configuration turns out to be lowest in energy.

We have performed first-principles density functional calculations with the projected augmented wave potential,<sup>9</sup> as implemented in the VASP,<sup>10</sup> using generalized gradient approximation<sup>11</sup> for the exchange-correlation energy. The plane wave basis set is used with kinetic energy cutoff of 300 eV. For Mn and Ni, 3*d* and 4*s* are considered as valence electrons. In case of Ce, 4*f*, 5*d*, and 6*s* are considered as valence electrons, while 5*s* and 5*p* are treated as semicore states. Brillouin zone sampling is performed using the Monkhorst-Pack method, with  $8 \times 8 \times 8$  **k** mesh for cubic and  $4 \times 6 \times 8$  **k** mesh for orthorhombic phases. **k** convergence has been established within an accuracy of 0.001 eV. The conjugate gradient method has been used to optimize the structures without any symmetry constraints. The structures are considered to be converged when the force on each ion becomes 0.001 eV/Å or less. This level of accuracy is also necessary to differentiate between closely lying various magnetic phases, such as ferromagnetic (FM), ferrimagnetic (FiM), antiferromagnetic (AFM).

Cubic CeMnNi<sub>4</sub> structure with space group  $F\bar{4}3m$  has already been described in earlier works.<sup>1-3</sup> The fcc unit cell (AuBe<sub>5</sub> structure) with lattice constant of 6.99 Å contains 4 f.u. with the Wyckoff positions Ce (0,0,0), Mn (1/4,1/4,1/4), and Ni (5/8,5/8,5/8), the latter forming corner-shared tetrahedra [Fig. 1(a)]. Another phase can be constructed from hexagonal CeNi<sub>5</sub> (CaCu<sub>5</sub> structure, space group *P6/mmm*) by substitution of Mn atom into any of the

<sup>a)</sup>Electronic mail: pmu@imr.edu

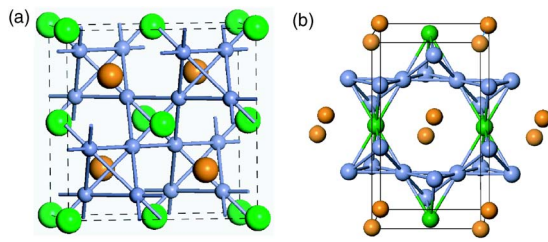


FIG. 1. (Color online) (a) Cubic and (b) orthorhombic structures of  $\text{CeMnNi}_4$ . The latter is derived from the hexagonal structure of the original  $\text{CeNi}_5$  structure. Orthorhombic lattices are marked as black colored boundary. Ce, Ni, and Mn atoms are represented by the orange, violet, and green colored balls, respectively.

Ni sites,  $2c(2/3, 1/3, 0)$  or  $3g(1/2, 1/2, 1/2)$ . But, the Mn atom prefers to occupy the  $3g$  rather than the  $2c$  site, as observed in the case of  $\text{LaMnNi}_4$ .<sup>12</sup> However, on substitution of Mn in one of the  $3g$  positions, the symmetry reduces from  $D_{6h}$  to  $D_{2h}$  and the new structure becomes orthorhombic (space group  $Cmmm$ ). In Fig. 1(b), we have shown how this orthorhombic unit cell can be generated from the parent hexagonal structure of  $\text{CeNi}_5$ . The orthorhombic phase has 2 f.u. with lattice parameters  $(a, b, c)$ , where  $a \approx \sqrt{(3)b}$ .

Figure 2 shows the energetics of all these magnetic as well as nonmagnetic (NM) phases for cubic and orthorhombic structures. It is found that NM state of cubic  $\text{CeMnNi}_4$  is unstable with respect to FM state (reduction in energy by  $\approx 0.7$  eV/f.u.), coupled with a concomitant increase in the unit cell volume (by  $\sim 6\%$ ) which corresponds to an increase in lattice parameter (i.e., negative pressure) from  $6.85 \text{ \AA}$  (for NM) to  $6.99 \text{ \AA}$  (for all magnetic phases). Note that the lattice parameter for cubic  $\text{CeNi}_5$  is  $\approx 6.91 \text{ \AA}$ ,<sup>4</sup> which is intermediate between the two above mentioned values. While all the cubic magnetic phases are bunched together, the FM phase lies lowest in energy compared to AFM and FiM phases (energy gains are 47 and 34 meV/f.u. with respect to AFM and FiM, respectively). This result is consistent with the experimental findings<sup>1</sup> as well as the earlier theoretical results.<sup>2,3</sup> But what we find most remarkable is that the total energy of orthorhombic phase is significantly lower than the cubic case (by 0.26 eV). This large energy difference in favor of the orthorhombic structure is startling, and we have tried to understand the reason for this discrepancy with the

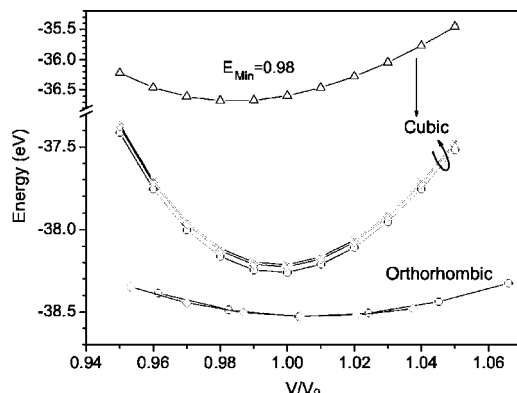


FIG. 2. Total energies per f.u. of  $\text{CeMnNi}_4$  for different structural and magnetic phases as function of volume ( $V/V_0$ , where  $V_0$  is equilibrium volume of cubic phase) are shown. In cubic phase, triangle, circle, rhombus, and cross symbols correspond to NM, FM, FiM, and AFM phases, respectively. For the orthorhombic phase (FM configuration), circle and rhombus symbols correspond to fixed  $b/a$  and  $c/a$ , respectively.

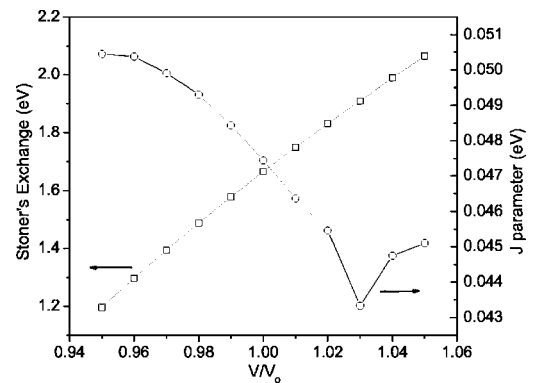


FIG. 3. Stoner and  $J$  values are shown as function of volume for cubic  $\text{CeMnNi}_4$ .

experimental finding. Moreover, we could not observe any possible pressure induced structural phase transition between orthorhombic and cubic phases. The equilibrium cell volumes are nearly same for both the phases, and the optimized lattice parameters for orthorhombic phase are  $a=8.43 \text{ \AA}$ ,  $b/a=0.60$ , and  $c/a=0.48$ .

For the AFM, FiM, and FM configurations, the calculated total magnetic moments are respectively 0.0, 2.49, and  $4.85 \mu_B/\text{f.u.}$ , which scale with the lowering in the corresponding total energies. This is reminiscent of the Stoner magnetism.<sup>13</sup> In Fig. 3, we plot the exchange coupling parameter ( $J$ ) defined as the energy difference between the AFM and FM states, and the Stoner's exchange is related to the energy difference between the NM and FM states. The  $J$  value decreases with increasing lattice parameter (Fig. 3). It shows that all magnetic phases do not change their states with variation of the cubic lattice parameter. In orthorhombic phase, the total magnetic moment of  $3.73 \mu_B/\text{f.u.}$  is lower than that of the cubic phase ( $4.85 \mu_B/\text{f.u.}$ ). However, this moment is much higher than the value  $0.42 \mu_B/\text{f.u.}$  reported for the hexagonal  $\text{CeMn}_x\text{Ni}_{5-x}$  ( $x=0.75$ ).<sup>5</sup> To understand further, we analyze the local moment contributions from each atomic species. We find the average local moments of Mn, Ni, and Ce for cubic (orthorhombic) phase as 3.96 (2.93), 0.28 (0.33), and  $-0.23$  ( $-0.46$ )  $\mu_B$ , respectively. The magnetism in both cubic and orthorhombic phases of  $\text{CeMnNi}_4$  mostly originates from Mn atoms. Large moment on Mn atoms in both phases induces some small moments (of opposite sign) in Ce and Ni atoms, as also shown in Ref. 5. The local moment on Mn atoms for the orthorhombic phase is significantly quenched due to shorter Mn-Ni distance ( $\sim 2.5 \text{ \AA}$ ), as compared to the cubic phase ( $\sim 2.9 \text{ \AA}$ ), and this in turn gets reflected on the total magnetic moment.

Now, coming to the analysis of the total and partial (site-projected) density of states (DOS) as shown in Figs. 3(a) and 3(b), we find the following salient features, viz., (a) large spin splitting of the Mn bands, (b) Ni bands almost completely filled, (c) Ce bands mostly unoccupied, but with the down-spin bands closer to  $E_F$  thereby contributing differently to the DOS, and (d) existence of pseudogap at  $E_F$  for cubic DOS. However, there are several distinguishing features between the DOSs for cubic and orthorhombic phases. First of all, we see that the Mn  $d$  bands for the two phases are quite different in the sense that the down-spin states for orthorhombic structure has a much longer tailing into the occupied band as compared to the cubic case. This is due to

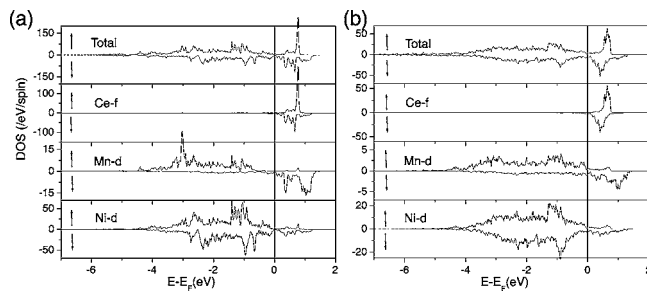


FIG. 4. Spin-polarized total and partial DOS for FM  $\text{CeMnNi}_4$  in (a) cubic and (b) orthorhombic phases. The up- and down-spin states are shown by arrow. Fermi level is shown by vertical line.

the different near-neighbor environment of Mn in the two structures. The Ce up and down bands are also seen to have different tailing behavior and hence have different contributions to the DOS at  $E_F$  for cubic and orthorhombic phases. It is important to discuss the hybridization between the Ni- $d$  and Mn- $d$  orbitals. The prominent Mn- $d$  peaks at  $-3.0$  eV (up-spin component) and at  $0.5$  eV (down-spin component) for cubic phase become much less pronounced for orthorhombic case. This indicates a strong  $d$ - $d$  hybridization for orthorhombic phase, resulting in a lower total energy, as compared to the cubic phase.

The origin of FM alignment of Mn atoms in  $\text{CeMnNi}_4$  is explained as follows. The Mn-Mn separations in cubic and orthorhombic phases are  $4.94$  and  $4.12$  Å, respectively. Such large values are indicative of indirect exchange interactions via the neighboring Ce or Ni atoms and that could be origin of FM coupling in Mn atoms. The bond distances of Ni-Mn and Ce-Mn for cubic (orthorhombic) phase are  $2.9$  Å ( $2.5$  Å) and  $3.03$  Å ( $3.21$  Å), respectively. The  $J$  value for cubic phase at equilibrium volume is  $47$  meV/f.u., which is larger than that for orthorhombic phase,  $10$  meV/f.u. It is known that  $J$  reduces rapidly with increasing bond distance.<sup>14</sup> Even though Ni-Mn bond for orthorhombic phase is shorter compared to cubic phase, we get a smaller  $J$  value for the former. On the other hand, Ce-Mn distance is smaller for cubic phase that results into larger  $J$  value compared to orthorhombic phase. Thus it is the Ce atoms, rather than Ni atoms, which are playing significant role in FM alignments of Mn atoms.

PCAR experiment<sup>1</sup> on cubic phase shows large degree of spin polarization of about 66%, indicating the possibility of achieving half-metallic nature. However, our first-principles study reveals metallic nature for both cubic and orthorhombic phases, albeit with the presence of some pseudogap (Fig. 4). The metallic behavior is stronger for orthorhombic as compared to cubic phase of  $\text{CeMnNi}_4$ . In Fig. 5 we show the band structures for cubic and orthorhombic phases, plotted along the high-symmetry directions. For cubic phase, the dispersion bands along the different symmetry directions are in quite good agreement with the other reports.<sup>2,3</sup> The degeneracies at the  $\Gamma$  point are mainly responsible for destroying the half metallicity. On the other hand, the possibility of half metallicity in orthorhombic phase appears to be remote [Fig. 5(b)]. The exact experimental conditions for synthesis of the

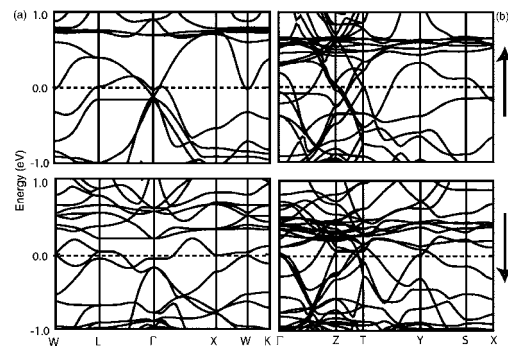


FIG. 5. Band structures of (a) cubic and (b) orthorhombic phases of FM  $\text{CeMnNi}_4$ . The up- and down-spin states are shown by arrow.

sample is still not completely understood, and the growth environment is likely to introduce small concentration of impurities or off-stoichiometric compositions that drive the system towards the stabilization of cubic phase, rather than the orthorhombic phase.<sup>2</sup>

In summary, we study the structural and magnetic stabilities of the cubic and orthorhombic phases of  $\text{CeMnNi}_4$  with various lattice parameters and possible magnetic and nonmagnetic configurations. Our results for cubic phase are in good agreement with earlier works.<sup>2,3</sup> Interestingly, the experimentally observed cubic phase lies higher in energy with respect to orthorhombic phase by  $0.26$  eV/f.u. We find ferromagnetic configuration to be stable for both the phases of  $\text{CeMnNi}_4$ , and the magnetic moment is mainly contributed by Mn atoms. The origin of FM alignment in Mn atoms is mediated via indirect exchange interaction. The DOS shows that both of the phases are metallic, rather than half metallic as proposed by experiment. However, there is a finite possibility of transforming it into complete half-metallic phase by engineering the electronic structure with introduction of some impurities. Also our study rules out any possibility of phase transition among the structural and magnetic phases, which demands further analysis of experimental samples.

<sup>1</sup>S. Singh, G. Sheet, P. Raychaudhuri, and S. K. Dhar, Appl. Phys. Lett. **88**, 022506 (2005).

<sup>2</sup>I. I. Mazin, Phys. Rev. B **73**, 012415 (2006).

<sup>3</sup>E. N. Voloshina, Y. S. Dedkov, M. Richter, and P. Zahn, Phys. Rev. B **73**, 144412 (2006).

<sup>4</sup>Ya. M. Kalychak, O. I. Bodak, and E. I. Gladyshevskii, Inorg. Mater. **12**, 961 (1976) [Izv. Akad. Nauk SSSR, Neorg. Mater. **12**, 1149 (1976)].

<sup>5</sup>F. Pourarian, M. Z. Liu, B. Z. Lu, M. Q. Huang, and W. E. Wallace, J. Solid State Chem. **65**, 111 (1986).

<sup>6</sup>N. Marcano, J. I. Espeso, J. C. Gomez Sal, J. R. Fernandez, J. H. Albillos, and F. Bartolome, Phys. Rev. B **71**, 134401 (2005).

<sup>7</sup>J. Tang and L. Li, J. Alloys Compd. **207-208**, 241 (1994).

<sup>8</sup>H. Flandorfer, P. Rogl, K. Hiebl, E. Bauer, A. Lindbaum, E. Gratz, C. Godart, D. Gignoux, and D. Schmitt, Phys. Rev. B **50**, 15527 (1994).

<sup>9</sup>P. E. Blochl, Phys. Rev. B **50**, 17953 (1994).

<sup>10</sup>Vienna *ab initio* software packages (VASP), <http://cms.mpi.univie.ac.at/vasp/>

<sup>11</sup>J. P. Perdew, J. A. Chevary, S. H. Vosko, K. A. Jackson, M. R. Pederson, D. J. Singh, and C. Fiolhais, Phys. Rev. B **46**, 6671 (1992).

<sup>12</sup>C. Lartigue, A. Percheron-Guégan, and J. C. Achard, J. Less-Common Met. **75**, 23 (1980).

<sup>13</sup>E. C. Stoner, Proc. R. Soc. London, Ser. A **169**, 339 (1939).

<sup>14</sup>J. B. Goodenough, *Magnetism and the Chemical Bond* (Interscience, New York, 1963).